Published in final edited form as:
Auton Neurosci. 2011 February 24; 160(1-2): 21–26. doi:10.1016/j.autneu.2010.10.010.

Ultrastructural Evidence for Selective GABAergic Innervation of CNS Vagal Projections to the Antrum of the Rat

Rebecca J. Pearson[1], **Philip J. Gatti**[2,3], **Niaz Sahibzada**[1], **V. John Massari**[2], and **Richard A. Gillis**[1]

[1]Departments of Pharmacology, Georgetown University Medical Center, Washington, DC

[2]Departments of Pharmacology, Howard University College of Medicine, Washington, DC

[3]Departments of Pharmacology, FDA/CDER, Division of Cardiorenal Products, Silver Spring, MD

Abstract

We reported pharmacological data suggesting that stimulation of a vago-vagal reflex activates GABAergic neurons in the hindbrain that inhibit dorsal motor nucleus of the vagus (DMV) neurons projecting to the antrum, but not to the fundus (Ferreira et al., 2002). The purpose of this study was to use an ultrastructural approach to test the hypothesis that GABAergic terminals form synapses with DMV antrum-projecting neurons, but not with DMV fundus-projecting neurons. A retrograde tracer, CTB-HRP, was injected into the gastric smooth muscle of either the fundus or the antrum of anesthetized rats. Animals were re-anethetized 48 hours later and perfusion-fixed with acrolein and paraformaldehyde. Brainstems were processed histochemically for CTB-HRP, and immunocytochemically for glutamic acid decarboxylase isoenzyme 67 immunoreactivity (GAD67-IR) by dual-labeling electron microscopic methods. Most cell bodies and dendrites of neurons that were retrogradely labeled from the stomach occurred at the level of the area postrema. Examination of 214 synapses on 195 neurons that projected to the antrum revealed that 23.0 +/− 3.6% (n=4) of synaptic contacts were with GAD67-IR terminals. The examination of 220 synapses on 203 fundus-projecting neurons revealed that only 7.9 +/− 3.1% (n=4) of synaptic contacts were with GAD67-IR terminals. The difference between GAD67-IR synaptic contacts with antrum- and fundus-projecting neurons was statistically significant ($p < 0.05$). These data suggest that brainstem circuitry controlling the antrum involves GABAergic transmission.

INTRODUCTION

Functionally, the stomach can be divided into a proximal region (fundus plus one third of the corpus) and a distal region (remaining two-thirds of the gastric corpus, the antrum and the gastroduodenal junction), (Kelly, 1981). The proximal part is involved in the receipt and storage of ingested material (Kelly, 1981), and the distal part is involved in trituration and retention of solid material (Kelly, 1981). The proximal region, specifically the fundus and the distal region, specifically the antrum, display different types of contractions. The fundus contractions are primarily tonic and the antrum contractions are primarily phasic.

Corresponding Author: Richard A. Gillis, Department of Pharmacology, Georgetown University gillisr@georgetown.edu, 3900 Reservoir Rd., NW Phone: 202-687-1607, Washington, DC 20057 Fax: (202)-687-5390.

Awareness of these separate functions of the two regions of the stomach and the different types of contractions exhibited by the fundus and antrum has led to the findings that the relative role of each region is different in normal gastric emptying. The proximal region plays a major role in the emptying of a liquid meal, while the distal region plays a major role in the emptying of a solid meal (Halser, 1995). In functional dyspepsia, evidence suggests that the antral tone and contractions are reduced (Hveem et al., 1996; Eberl, 1998; Loreno et al., 2004, Troncon et al., 2006) while fundus tone is increased (Tack et al., 1998; Stranghellini et al., 2003, Di Stefano et al., 2005).

In view of the separation of function of the two regions of the stomach, and in view of evidence that these two regions operate independently depending on what type of meal is ingested and during periods of gastric dysfunction (e.g. functional dyspepsia), there must be separate regulatory mechanisms for controlling the fundus and antrum. A major controlling influence on the two regions are the vagus nerves (Kelly, 1981; Meyer, 1994), and these nerves have their origin in the hindbrain, i.e., in the dorsal motor nucleus of the vagus (DMV) (Gillis et al., 1989). Hence, a likely source for independent regulation of the fundus and antrum is the hindbrain, but, how can this be carried out by the neurocircuits present in this part of the brain?

This question was addressed in our recent publication (Pearson et al., 2007). It was addressed by determining whether afferent inputs to DMV projections to the fundus and antrum were different. Our hypothesis was that the afferent input to DMV fundus projecting neurons is noradrenergic. We tested our hypothesis by using electron microscopy and determining whether noradrenergic terminals form synapses with DMV fundus-projecting neurons. We reported visual evidence for the existence of synaptic contacts between fundus-projecting DMV neurons and dopamine beta hydroxylase (DBH) immunoreactive (IR) terminals. In addition, we found no synaptic contact between antrum projecting neurons and DBH-IR terminals.

The compelling next question that needs to be addressed is the nature of the inhibitory afferent input to DMV projection neurons innervating the antrum? A likely candidate is GABA based on electrophysiological evidence of our earlier study (Travagli et al., 1991) and the more recent study of Smith and colleagues (Davis et al., 2004). The purpose of the present study was to visualize GABAergic terminals with the antibody to glutamic acid decarboxylase type 67 (GAD67), and determine whether GABAergic terminals synapse with identified DMV antrum-projecting neurons. In addition, we also assessed whether GABAergic terminals synapse with DMV fundus-projecting neurons.

MATERIALS AND METHODS

Retrograde Tracing Studies

The materials and methods for retrograde tracing studies are described in detail in our previous study, (Pearson et al., 2007). The hindbrain tissue used to study noradrenergic innervation of CNS vagal projections to the fundus (and to the antrum) in our previous study reveal that the highest populations of antrum and fundus projecting neurons in the DMV is within the area between the calamus scriptorius (cs) to 0.5 mm rostral to cs. For the present study of GABAergic innervation of CNS vagal projections to the antrum and fundus of the rat, tissue was also taken from this area.

Briefly, unfasted, adult male Sprague-Dawley rats (275–325 g) (Taconic) were anesthetized with isoflurane (Fischer Scientific). The stomach was exposed and a 1% solution of cholera toxin conjugated to horseradish peroxidase [CTB-HRP, (List Biologicals)] was injected into

either the antrum or the fundus. [NOTE: details on volume of injectate and controls used appear in our earlier paper (Pearson et al., 2007)].

After a 48 hour survival period, animals were sacrificed under pentobarbital [60mg/kg, i.p., (Abbott Laboratories)] by transcardiac perfusion with fixative (paraformaldehyde and acrolein), and brainstems harvested and processed histochemically for CTB-HRP.

The number of animals used for the retrograde tracing studies was fifteen (antrum, n=7; fundus, n=8). Properly placed injections in the antrum and fundus were expected to- and did mimic, the results of Okumura and Namiki (1999), and Pagani et al. (1988). Both of these investigators note a consistent medial-lateral distribution of retrogradely labeled neurons with antrum-projecting neurons located more medial than fundus-projecting neurons, and our results are similar (Pearson et al., 2007).

CTB-HRP Histochemistry

These materials and methods were described previously in our paper (Pearson et al., 2007), and are repeated here because of our need to provide information that will enable an objective evaluation of our ultrastructural data on GABAergic neurons innervating DMV projections to the antrum and fundus.

Brainstems were sectioned on either a Leica SM2000R sliding microtome (Leica Instruments) into 25um coronal sections for light microscopic analysis or a Vibratome Series 1000 sectioning system (Technical Products International, Inc.) into 40um coronal sections for electron microscopy. Free-floating sections were processed to identify CTB-HRP labeled entities by the tungstate stabilized tetramethylbenzidine (TMB) method of Weinberg and Van Eyck (1991), as described in detail by Llewellyn-Smith and Minson (1992). This method was performed at pH 6.0 and yields a crystalline reaction product which is readily detected in the electron microscope. Sections were pre-incubated for 20 minutes in a solution containing: 100ml of 0.1 M PBS, pH 6.0; 5.0 ml 1% ammonium paratungstate; 1.0 ml of 0.4% NH4CL; 1.0 ml 20% D-glucose; and 1.25 ml of 0.2% TMB free base in ethanol. Subsequently, the sections were incubated in 100 ml of the same solution with the addition of 600 International Units (IU) of glucose oxidase. The development of the blue reaction product which is formed by the glucose oxidase reaction was monitored under a dissecting microscope and is typically complete within 20–30 minutes. The sections were washed 3 times in fresh 0.1 M phosphate buffer, pH 6.0, and then the reaction product was stabilized and enhanced with a cobalt chloride diaminobenzidine-glucose oxidase reaction in a minor variation on the method of Rye et al. (1984). Briefly, tissues were incubated for 7 minutes in a solution containing: 100 ml 0.1 M phosphate buffer, pH 6.0; 100 mg diaminobenzidine (DAB); 1.0 ml NH4CL; 1.0 ml of 20% D-glucose; 2.0 ml of 1% cobalt chloride in water; and 600 IU of glucose oxidase. This second glucose oxidase reaction was terminated by washing in excess sodium phosphate buffer. Sections for light microscopy (25um) were rinsed with PBS and mounted on glass slides for analysis. To analyze the distribution of antrum or fundus projecting neurons, neurons in every 5th section were counted and a total of labeled neurons for each animal was averaged and plotted. Sections processed for electron microscopy were rinsed in PBS and then processed immunocytochemically for the presence of gamma amino butyric acid (GAD67).

Immunocytochemistry

The GAD67 monoclonal antibody (MAB5406) was purchased from Chemicon (Temecula, CA). The secondary antibody (biotinylated anti-mouse, made in horse, was purchased from

Vector Laboratories (Burlingame, CA). MAB5406 was chosen because it was used successfully in ultrastructural studies (Moore et al., 2004; Fong et al., 2005).

Controls were done to test the ability of MAB5406 to selectively label GAD67 containing terminals. Two controls involved using hindbrain tissue that underwent all the same tissue processing protocols to detect GAD67-IR except the tissue was not exposed to either the primary antibody (one control group) or the secondary antibody (second control group). When either antibody was missing, neurons were not labeled. The third control involved using hindbrain tissue that had undergone the protocol (described below), tissue was then exposed to the GAD67 antibody, and was examined for distribution patterns reported by Fong et al., 2004. Thus, like Fong et al., 2004, we found GAD67-IR in the perikarya of neurons of the NTS, the area postrema (AP), and the ventrolateral medulla, but not in the perikarya of neurons in the DMV and in the hypoglossal nucleus.

Brainstem sections were incubated for 30 minutes in a solution of 50% absolute ethanol in distilled water to enhance the penetration of antibodies throughout the tissue, followed by 3 washes in PBS. Tissues were then incubated in 0.1M PBS containing 1.0% bovine serum albumin (BSA) for 30 minutes and then incubated overnight in primary antibody. The primary antibody was washed out the following morning by 3 washes in 0.1% PBS-BSA and the tissues were then incubated for one hour in secondary antibody. Sections were rinsed in PBS-BSA (0.1%) and then incubated for 1 hour in avidin-biotin peroxidase complex [1:50 in 0.1% PBS-BSA using the Vectastain ABC Elite kit followed by a glucose oxidase reaction utilizing DAB (100 mg DAB, 0.04% NH_4Cl, 0.2% D-glucose, 1200 IU glucose oxidase in 0.1M PBS)] to visualize the product. This reaction yields an amorphous electron dense reaction product when viewed in the electron microscope.

Processing for Electron Microscopy

Sections containing CTB-HRP-labeled cells were processed for electron microscopy. These sections were further preserved in 2% osmium tetroxide for 1 hour, and rinsed with PBS. Free-floating sections were exposed to a graded series of dehydrations in ethanol and propylene oxide, and incubated overnight in a 1:1 propylene oxide:epon 812 plastic resin solution (Electron Microscopy Sciences). Tissues were flat-embedded between 2 sheets of aclar plastic (Ted Pella) and heated for 48 hours at 60° C. Embedded tissues were examined under a light microscope and the area of interest, the DMV, was cut out and re-embedded in Beem capsules which were filled with freshly prepared Epon 812 and heated for 48–72 hours at 60°C. The hardened samples were removed from the oven and blocked for ultramicrotomy under a dissecting microscope (Nikon SMZ-U, Zoom 1–10). Blocks were cut on a Reichert Ultracut S ultramicrotome (Reichert, Leica Microsystems) into 70nm serial sections which were captured onto 300 mesh copper grids (Electron Microscopy Sciences) and double stained with uranyl acetate and lead citrate using a Leica EMStain Ultrastainer (Leica Microsystems). Sections were examined in a JEOL-JEM-1210 transmission electron microscope at 50 or 80 kV accelerating voltage.

Two 40um sections from the intermediate DMV (this area includes DMV tissue beginning at the cs on the caudal end and extending +0.5 mm rostral) containing retrogradely labeled neurons from either the fundus or the antrum were examined. These sections were chosen because they contained the best combination of morphological preservation and histochemical/ immunocytochemical labeling from each animal. From each 40 um-thick section, 3 ultrathin sections separated by ~12 um each were utilized for subsequent quantitative analysis. The spatial separation provided between samples insured the prevention of duplicate counts of the same terminal in our 3 samples throughout the neuropil. Ultrathin sections were examined at 8,000x magnification for the presence of the tungstate-TMB-generated crystalline reaction product. All retrogradely labeled profiles were

photographed at 8,000x and 20,000x magnification. Synaptic contacts were examined in 20,000x magnification photographs taken of the entire circumference of all retrogradely labeled profiles. Photographic images were recorded using a Gatan Model 895 Ultra Scan 4000 CCD camera (Gatan, Warrendale, PA). Neuronal and dendritic profiles were identified according to previous ultrastructural descriptions (Peters et al., 1999; Gray, 1959, Massari et al., 2002). All terminals that made synaptic contact with retrogradely labeled neurons were identified and categorized as 'labeled' or 'unlabeled' based on the presence or absence of GAD67-IR in the terminal. These terminals were further characterized as either synaptic contacts or appositions. A synaptic contact is characterized by the presence of an electron-dense post-synaptic density and a pre-synaptic terminal with immunocytochemically-labeled vesicles which are located near the terminal membrane where it directly contacts the post-synaptic density. For each GAD67-IR terminal examined, an unlabeled terminal in close proximity was visually compared with it to establish a level of background. Terminals varied in intensity of GAD67 label but only terminals that were obviously darker than all the terminals in the surrounding areas of the section were counted as 'GAD67-IR'. Appositions are an immunoreactive terminal which is closely juxtaposed to a CTB-HRP-labeled profile but doesn't possess an electron-dense post-synaptic density. Each contact was then identified as either 'axo-somatic' or 'axo-dendritic' and either symmetric or asymmetric based on previously reported definitions (Peters et al., 1999).

The total number of profiles which contained CTB-HRP retrograde labeling is expressed in Table 1 and is the combined total of each animal added together. The same method was used to obtain figures for the total synaptic contacts and total appositions shown in Table 1. The percent of synapses (or appositions) formed between retrogradely labeled profiles and immunoreactive terminals was calculated for each animal from a total of the synaptic contacts for that animal. The individual percentages for each animal were then averaged with the percentages of other animals in the experimental group to yield the data expressed in Table 1 (GAD67-IR with antrum or fundus-projecting neurons). Average values for these data are presented as means +/− SEM. Statistical comparisons were made using the Student's t-test. The criterion for statistical significance was $p < 0.05$.

5. RESULTS

5.1 Light microscopic analysis of the DMV after injection of CTB-HRP into either the antrum or the fundus

Our first step in performing electron microscopic analyses of GABAergic terminals synapsing onto DMV neurons that project either to the antrum or to the fundus was to locate the portion (or portions) of the DMV that contained the highest density of these stomach projecting preganglionic vagal neurons. This step was carried out for our previous study of noradrenergic innervation of CNS vagal projections to the fundus and to the antrum (Pearson et al., 2007), and we refer to those findings. Most cell bodies and dendrites of neurons that were retrogradely labeled from the antrum (n=7) and fundus (n=8) occurred at the level of the area postrema. The DMV was the only brainstem area to be labeled by CTB-HRP injection into the antrum and into the fundus. For the antrum, 80% of all labeled DMV neurons were contained in the area between calamus scriptorius (cs) and 0.75 mm rostral to cs (i.e., within a 750 um span of the DMV). For the fundus, 80% of all labeled DMV neurons were contained in the area −0.125 to + 0.5 mm on either side of the cs (i.e., within a 625 um span of the DMV). Thus, based on our earlier data (Pearson et al., 2007), the area from cs to + 0.5 mm rostral to the cs is the region of the DMV where ultrathin sections were taken for electron microscopic analyses of GABAergic synapses.

5.2 Electron Microscopic Analyses

GAD67-IR was found in the DMV within the area containing the largest population of CTB-HRP from the antrum and the fundus. Immunoreactivity could be identified as an electron-dense, amorphous DAB reaction product in the electron microscope, and was found primarily in nerve terminals as well as in some unmyelinated axons. GAD67-IR terminals (Fig. 1a and 1b) formed both axo-dendritic and axo-somatic synaptic contacts with CTB-HRP labeled dendrites and perikarya, as well as many appositions (Table 1). [NOTE: retrograde label from CTB-HRP injected into the antrum or fundus was readily observed in perikarya, proximal and distal dendrites, and myelinated axons by the presence of a crystalline TMB-tungstate reaction product (Fig. 2; also Fig. 3a and 3b)]. GAD67-IR terminals contained an assortment of numerous small, clear, and primarily round vesicles (Fig. 1a), although a few also contained pleomorphic vesicles (Fig. 1b). A small number of GAD67-IR terminals were observed to also contain large, dense core vesicles. GAD67-IR terminals formed mostly symmetric synapses, although a few asymmetric synapses were also observed. From a pooled total of 214 synaptic contacts with retrogradely labeled dendritic and somatic profiles from the antrum, 23.0 +/− 3.6% were GAD67-IR (Table 1). The proportion of GAD67-IR terminals that formed axo-dendritic synapses [approximately 93.5%, (fig. 2a)] was significantly higher than the proportion that formed axo-somatic synapses (approximately 6.5%), ($p < 0.05$). The percentage of 23.0 +/− 3.6% may have been an under-estimation because the examination of the brain tissue revealed many appositions with retrogradely labeled profiles, and the percent of appositions with GAD67-IR was 19.9 +/− 6.3% (Table 1).

From a pooled total of 220 synaptic contacts with retrogradely labeled dendritic and somatic profiles from the fundus, 7.9 +/− 3.1% were GAD67-IR (Table 1). This percentage is significantly less ($p < 0.05$) than the 23.0 +/− 3.6% of synapses formed between GAD67-IR terminals and antrum projecting neurons. The proportion of GAD67-IR terminals that formed axo-dendritic synapses [approximately 94.7%, (Fig. 3a)] was significantly higher than the proportion that formed axo-somatic synapses (approximately 5.3 %), ($p < 0.05$). An example of synaptic contact between a CTB-HRP labeled dendrite and a GAD67-IR terminal can be seen in Fig. 3a. The percentage of 7.9 +/− 3.1% may be an under-estimation because the examination of the brain tissue revealed many appositions with retrogradely labeled profiles, and the percent of appositions with GAD67-IR was 17.4 +/− 3.4% (Table 1). Many synaptic contacts were observed between CTB-HRP labeled dendrites and unlabeled terminals (Fig. 3b).

6. DISCUSSION

The purpose of our study was to visualize GABAergic terminals with the antibody to GAD67 and assess ultrastructurally whether GABAergic terminals synapse with DMV antrum projecting neurons. The vast majority of synaptic contacts between antrum projecting profiles and GAD67 terminals were axo-dendritic and were of the symmetric (or inhibitory) type. The GAD67-IR terminals observed contained an assortment of numerous small, clear, and primarily round vesicles. A few terminals also contained pleomorphic vesicles. These types of vesicles are known to accumulate and store fast-acting neurotransmitters such as GABA (Torrealba and Carrasco, 2004). In the quantitative analysis of neurons which project to the antrum we found that of all the synapses observed with these neurons, 23.0 +/− 3.6% contained GAD67-IR. This percentage is very similar to data of others (Moore et al., 2004) who reported findings on GAD-IR terminals synapsing with airway-related vagal preganglionic neurons (AVPNs) in the rostral nucleus ambiguous. From all of the synaptic contacts with retrogradely labeled AVPNs, 20.2% were GAD-IR.

A question raised by our data is whether a percentage value of 23.0 +/− 3.6% of the synapses onto DMV antrum projecting neurons is enough to play a physiological role in communicating signals within a portion of the vago-vagal reflex pathway? Though this question cannot be directly resolved using electron microscopy alone, data from our previous study, (Ferreira et al., 2002), demonstrate a functional correlation to this structural study. We reported, (Ferreira et al., 2002), that nicotine-induced activation of NTS neurons in the rat inhibited phasic contractions recorded from the antrum. This inhibitory effect of NTS stimulation was concluded to be due to locally applied nicotine activating second-order neurons in a vago-vagal reflex pathway which, in turn, inhibited DMV antrum projecting neurons. Most important, approximately 80% of the nicotine-induced inhibition of antrum phasic contractions was blocked by microinjection of a GABAa receptor antagonist into the DMV. Thus, since the largest part of the nicotine-induced inhibition of antrum phasic contractions was counteracted by GABAa receptor blockade at the DMV, we conclude that activity in only 23.0 +/– 3.6% of the synapses is sufficient to evoke a physiological response.

In contrast, we found relatively fewer synaptic contacts between fundus projecting neurons and GAD67-IR terminals. In our quantitative analysis of neurons, which project to the fundus, we found that of all the synapses observed with these neurons, only 7.9 +/– 3.1% were GAD67-IR. As in the case of the antrum projecting neurons, synapses were of the symmetric type and the majority were axo-dendritic synapses. Is activity communicated by just 7.9 +/– 3.1% of the total number of synapses sufficient to produce a physiological response? We conclude that in the case of nicotine-induced inhibition of fundus tone produced from the NTS, it is not. We conclude this based on our earlier finding that blockade of GABAa receptors at the DMV does not affect nicotine-induced inhibition of fundus tone mediated by a DMV vagal projection to the fundus (Ferreira et al., 2002).

In summary, our data indicate that the CNS has the capacity to provide region-specific control over the antrum and fundus through engaging phenotypically different afferent inputs to the DMV. In the case of the antrum, as suggested by data in the present study, a GABAergic projection is engaged, while in the case of the fundus, a noradrenergic projection is engaged (see our previous paper; Pearson et al., 2007). Finally, our data demonstrating that GAD67-IR terminals make contact with antrum projecting neurons are consistent with “wiring’ transmission at the DMV (Agnati et al., 1995).

Additionally, we quantitatively analyzed the terminals which formed appositions with the retrogradely-labeled antrum projecting profiles and found 19.9 +/− 6.3% were positive for GAD-IR. Terminals which formed appositions with retrogradely-labeled fundus projecting neurons were found to be GAD-IR in 17.4 +/− 3.4 % cases. Appositions are terminals which may make a synaptic contact at a different plane of view, and therefore, lead us to the speculation that the number of synaptic contacts observed may be an under-estimation. However, because there is no discernable pre- or post-synaptic density evident in the case of these profiles, their physiological significance is uncertain.

The source of GABAergic input to antrum projecting neurons was not determined in our study but would be important to determine so that knowledge of more of the vagovagal reflex circuitry could be realized. Also, knowledge of the source would put us in a position where we could search for the afferent inputs to GABAergic neurons synapsing onto DMV antrum projecting neurons. The most likely source is the medial subnucleus of the tractus solitarius (mNTS). Immunohistochemical localization studies of GAD67-expressing neurons and processes in the rat brainstem have revealed that the highest numbers of labeled cells are found in the mNTS (Fong et al., 2005). Most important, Davis and colleagues, 2004, have performed whole-cell patch clamp recordings from DMV neurons in rat brain slices while

using glutamate photostimulation to activate discrete areas of the NTS. With NTS stimulation, they observed that 65% of the DMV neurons exhibited IPSCs. These IPSCs were blocked by picrotoxin indicating that GABA mediated them. These investigators suggest, “there is a predominance of inhibitory projections to the DMV originating from intact neurons of the NTS.” This suggestion was based on the finding that IPSCs were more often found in DMV recordings than EPSCs.

Additional evidence that an important source of the GABAergic input to DMV antrum projecting neurons can be drawn from studies of a parallel system involving DMV preganglionic neurons projecting to the rat heart. Wang and colleagues, 2001, studied DMV cardiac projecting neurons in an in vitro slice preparation using patch clamp electrophysiology. These neurons displayed spontaneous IPSCs that were blocked by bicuculline. Tonic GABAergic input to DMV cardiac vagal neurons was approximately 3-fold higher than the tonic GABAergic input to nucleus ambiguus cardiac projecting neurons. To determine the source of the tonic GABAergic input, the NTS was electrically stimulated. Synaptic currents in DMV vagal neurons were consistently produced and these currents were blocked by bicuculline. Most important, NTS stimulation evoked responses which followed high frequency stimulation and exhibited a constant latency. These observations indicate the presence of a monosynaptic GABAergic pathway from the NTS to the DMV. It was also noted in this study that with accidental over-stimulation of the NTS, most of the NTS neurons appeared damaged. Under this condition, tonic GABAergic input to the DMV was decreased or abolished.

We also considered the possibility that a source of GABAergic input to antrum projecting neurons was from interneurons within the DMV. This, however, is an unlikely source based on Fong and colleagues’ observation in the rat that in contrast to the mNTS, no GAD67-IR cells were present in the DMV (Fong et al., 2005). On the other hand, GAD67-IR terminals were clearly present in the DMV.

In view of our findings that DMV antrum projecting neurons receive a significant GABAergic afferent input relative to the GABAergic afferent input to DMV fundus projecting neurons, coupled with Ferreira and colleagues’, 2002, data showing that bicuculline microinjected into the DMV counteracts nicotine-evoked inhibition of the antrum but not the nicotine-evoked inhibition of the fundus, it seems reasonable to predict that bicuculline microinjected into the DMV would increase antrum contractility but not fundus contractility. This prediction is compatible with data of two published studies but is in conflict with data of another published study. Referring to ‘compatible’ data, Ferreira et al., 2002, microinjected bicuculline, 25 pmol, bilaterally into the DMV of the rat and observed a statistically significant increase in antrum motility (+29.4 +/− 7.3 minute motility units, $p < 0.05$, n=6), but no statistically significant increase in fundus motility (+1.4 +/− 0.8 grams, $p > 0.05$, n=6). In their study, Washabau et al., 1995, observed an increase in antral muscle activity following bicuculline microinjection into the DMV of the cat in 36% of the DMV sites tested. This contrasted with an increase in fundic pressure following bicuculline microinjection in only 12% of DMV sites tested. Referring to ‘conflicting’ data, Sivarao and colleagues, 1998, observed significant increases in intragastric pressure with bicuculline microinjected into the rat dorsal vagal complex. [NOTE: an increase in intragastric pressure is an indication of an increase in fundus contractility]. The doses of bicuculline used for their studies was more than 14 fold higher than the dose of bicuculline used in the Ferreira et al., 2002, study. Dose-response data reported for microinjection-induced effects of bicuculline in the rat indicate that full responses will occur with microinjected amounts ranging between 2 and 20 pmol (Soltis and DiMicco, 1991). Hence, data published by Sivarao et al., 1998, are difficult to interpret because diffusion of such a high dose of bicuculline from the site of microinjection could

result in drug concentrations high enough to block GABAa receptors at sites outside the dorsal vagal complex.

In summary, our data indicate that DMV antrum projecting neurons receive significant GABAergic afferent input. This input, based on studies of others (eg. Fong et al., 2005; Davis et al., 2004; Wong et al., 2001) probably originates in the mNTS. This suggests that the GABAergic synapses at the DMV described in this study could be involved in mediating decreases in contractility of the antrum produced by activation of a vago-vagal reflex pathway.

Acknowledgments

Grant Support: NIH grant #'s: R01DK57105 (RAG), R01DK56925 (RAG), R24MH067627 (VJM), U54NS039407 (VJM), 2G12RR003048 (VJM), and F31NS049786 (RJP).

Abbreviations

GAD	glutamic acid decarboxlyase
IR	immunoreactive
DMV	dorsal motor nucleus of the vagus
NTS	nucleus tractus solitarius
mNTS	medial subnucleus of the tractus solitarius
cs	calamus scriptorius
CTB-HRP	cholera toxin beta subunit conjugated to horseradish peroxidase
DBH	dopamine-beta-hydroxylase
PNMT	phenylethanolamine-N-methyltransferase
TH	tyrosine hydroxylase

REFERENCES

1. Agnati LF, Zoli M, Stromberg I, Fuxe K. Intercellular communication in the brain: wiring versus volume transmission. Neurosci. 1995; 69:711–726.
2. Davis SF, Derbenev AV, Williams KW, Glatzer NR, Smith BN. Excitatory and inhibitory local circuit input to the rat dorsal motor nucleus of the vagus originating from the nucleus tractus solitarius. Brain Res. 2004; 1017(1–2):208–217. [PubMed: 15261116]
3. Di Stefano M, Micelli E, Mazzocchi S, Tana P, Corazza GG. The role of gastric accommodation in the pathophysiology of functional dyspepsia. Eur. Rev. Med. Pharmacol. Sci. 2005; 9:23–28. [PubMed: 16457126]
4. Eberl T, Barnert J, Dumitrascu DL, Fischer J, Weinbeck M. The effect of cisapride on dysmotility-like functional dyspepsia: reduction of the fasting and postprandial area, but not the postprandial antral expansion. Eur. J. Gastroenterol. Hepatol. 10:991–995. [PubMed: 9895043]
5. Ferreira M Jr, Sahibzada N, Shi M, Panico W, Neidringhaus M, Wasserman A, Kellar KJ, Verbalis J, Gillis RA. CNS site of action and brainstem circuitry responsible for the intravenous effects of nicotine on gastric tone. J. Neurosci. 2002; 22:2764–2779. [PubMed: 11923442]
6. Fong AY, Stornetta RL, Foley CM, Potts JT. Immunohistochemical localization of GAD67-expressing neurons and processes in the rat brainstem: distribution in the nucleus tractus solitarius. J. Comp. Neurol. 2005; 493:274–290. [PubMed: 16255028]
7. Gillis RA, Quest JA, Pagani FD, Norman WP. Control centers in the central nervous system for regulating gastrointestinal motility. Chapter 17. Handbook of Physiology: Vol. IV Gastrointestinal Motility and Circulation. 1989:621–683.

8. Gray EG. Axo-somatic and axo-dendritic synapses of the cerebral cortex: an electron microscopic study. J. Anat. 1959; 93:420–433. [PubMed: 13829103]
9. Hasler, WL. The physiology of gastric motility and gastric emptying. Chapter 8. In: Yamada, T., editor. Textbook of Gastroenterology. 2nd ed.. Philadelphia: Lippincott Company; 1995. p. 181-206.
10. Hveem K, Hausken T, Svebak S, Berstad A. Gastric antral motility in functional dyspepsia. Effect of mental stress and cisapride. Scand. J. Gastroenterol. 1996; 31:452–457. [PubMed: 8734341]
11. Kelly, KA. Motility of the Stomach and Gastroduodenal Junction. Chapter 12. In: Johnson, LR., editor. Physiology of the Gastrointestinal Tract. 1st ed.. Vol. Volume 1. New York: Raven Press; 1981. p. 393-410.
12. Llewellyn-Smith IJ, Minson JB. Complete penetration of antibodies into vibratome sections after glutaraldehyde fixation and ethanol treatment: light and electron microscopy for neuropeptides. J. Histochem. Cytochem. 1992; 40:1741–1749. [PubMed: 1431060]
13. Loreno M, Bucceri AM, Catalano F, Muratore LA, Blasi A, Brogna A. Pattern of gastric emptying in functional dyspepsia. An ultrasonographic study. Dig. Dis. Sci. 2004; 49:404–407.
14. Massari VJ, Haxhiu MA. Substance P afferent terminals innervate vagal preganglionic neurons projecting to the trachea of the ferret. Auton. Neurosci. 2002; 96:103–112. [PubMed: 11958475]
15. Mayer, EA. The physiology of gastric storage and emptying, Chapter 22. In: Johnson, LR., editor. Physiology of the Gastrointestinal Tract. 3rd ed.. Vol. Vol 1. New York: Raven Press; 1994. p. 929-977.
16. Moore CT, Wilson CG, Mayer CA, Acquah SS, Massari VJ, Haxhiu MA. A GABAergic inhibitory microcircuit controlling cholinergic outflow to the airways. J. Appl. Physiol. 2004; 96:260–270. [PubMed: 12972437]
17. Okumura T, Namiki M. Vagal motor neurons innervating the stomach are site-specifically organized in the dorsal motor nucleus of the vagus nerve in rats. J. Autonomic Nervous System. 1999; 29:157–162.
18. Pagani FD, Norman WP, Gillis RA. Medullary parasympathetic innervate specific sites in the feline stomach. Gastroenterology. 1988; 95:277–288. [PubMed: 3391362]
19. Pearson RJ, Gatti PJ, Sahibzada N, Massari VJ, Gillis RA. Ultrastructural evidence for selective noradrenergic innervation of CNS vagal projections to the fundus. Auton. Neurosci. 2007; 136(1–2):31–42. [PubMed: 17572158]
20. Peters, A.; Palay, SL.; Webster, HD. The Fine Structure of the Nervous System. New York: Oxford University Press; 1999.
21. Rye DB, Saper CB, Wainer BH. Stabilization of the tetramethylbenzidine (TMB) reaction product: application for retrograde and anterograde tracing, and combination with immunohistochemistry. J. Histochem. Cytochem. 1984; 32:1145–1153. [PubMed: 6548485]
22. Sivarao DV, Krowicki ZK, Hornby PJ. Role of GABAA receptors in rat hindbrain nuclei controlling gastric motor function. Neurogastroenterol. Mot. 1998; 10:305–313.
23. Soltis RP, Di Micco JA. GABAA and excitatory amino acid receptors in dorsomedial hypothalamus and heart rate in rats. Am. J. Physiol. 1991; 260:R13–R20. [PubMed: 1671541]
24. Stranghellini V, DePointi F, DeGiorgio R, Barbera G, Tosetti C, Corinaldesi R. New developments in the treatment of functional dyspepsia. Drugs. 2003; 63:869–892. [PubMed: 12678573]
25. Tack J, Piessevaux H, Coulie B, Caenepeel P, Janssens J. Role of impaired gastric accommodation to a meal in functional dyspepsia. Gastroenterology. 1998; 115:1346–1352. [PubMed: 9834261]
26. Torrealba F, Carrasco MA. A review on electron microscopy and neurotransmitter systems. Brain Res. 2004; 47:5–17.
27. Travagli RA, Gillis RA, Rossiter CD, Vicini S. Glutamate and GABA-mediated synaptic currents in neurons of the rat dorsal motor nucleus of the vagus. Am. J. Physiol. 1991; 260:G531–G536. [PubMed: 1672243]
28. Troncon LE, Herculano JR Jr, Savoldelli RD, Moraes ER, Secaf M, Oliveira RB. Relationships between intragastric food maldistribution, disturbances of antral contractility, and symptoms in functional dyspepsia. Dig. Dis. Sci. 2006; 51:517–526. [PubMed: 16614961]

29. Wang J, Irnaten M, Mendelowitz D. Characteristics of spontaneous and evoked GABAergic synaptic currents in cardiac vagal neurons in rats. Brain Res. 2001; 889:78–83. [PubMed: 11166689]

30. Washabau RJ, Fudge M, Price WJ, Barone FC. GABA receptors in the dorsal motor nucleus of the vagus influence feline lower esophageal sphincter and gastric function. Brain Res. Bull. 1995; 38:587–594. [PubMed: 8590083]

31. Weinberg WJ, van Eyck SL. A tetramethylbenzidine/tungstate reaction for horseradish peroxidase histochemistry. J. Histochem. Cytochem. 1991; 38:1143–1148. [PubMed: 1906909]

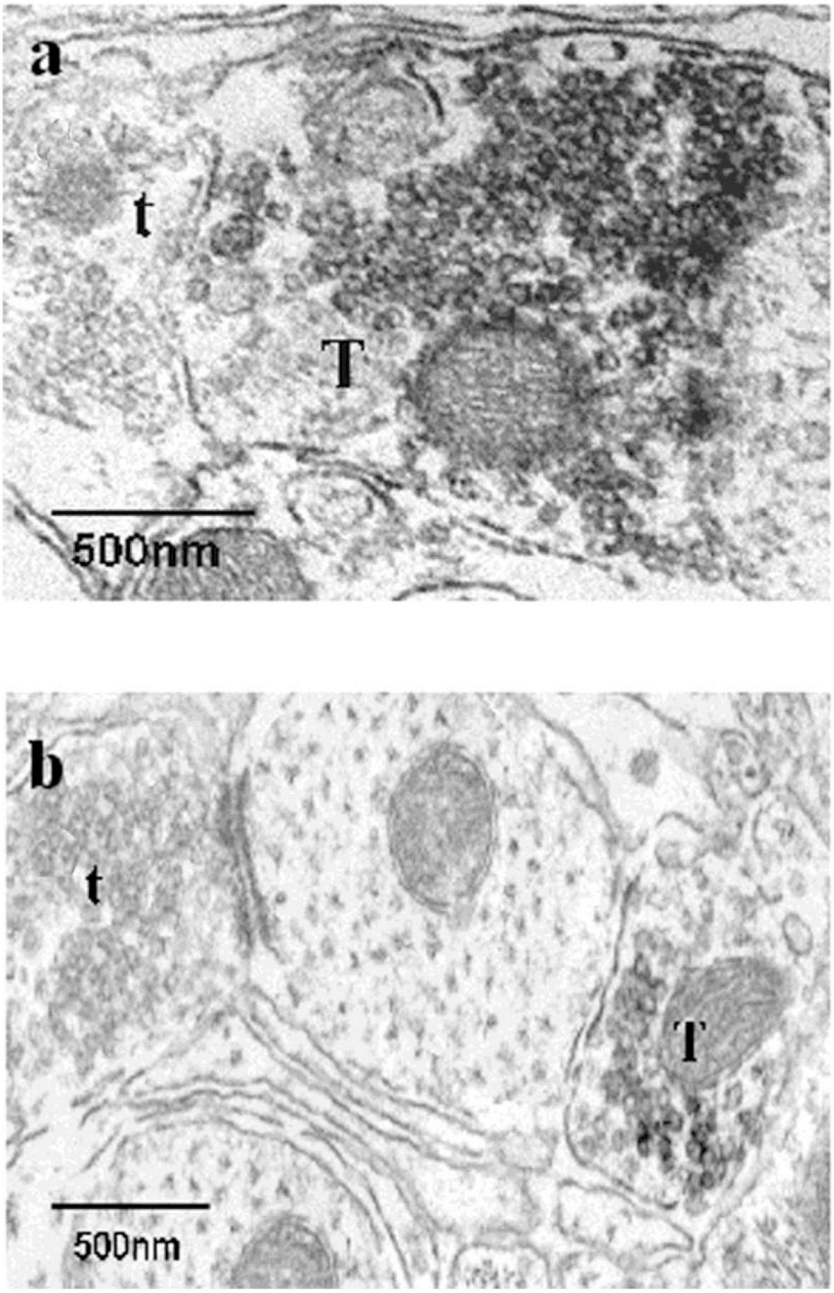

Figure 1.
GAD67-IR at the ultrastructural level. GAD67-IR is readily detected as a dark, amorphous, diaminobenzidine (DAB) reaction product (1a, 1b). Note that the GAD67-IR terminal (T) contains a population of small, clear, round vesicles (1a) though some pleomorphic vesicles were occasionally observed (1b). Unlabeled terminals (t) are identified for comparison.

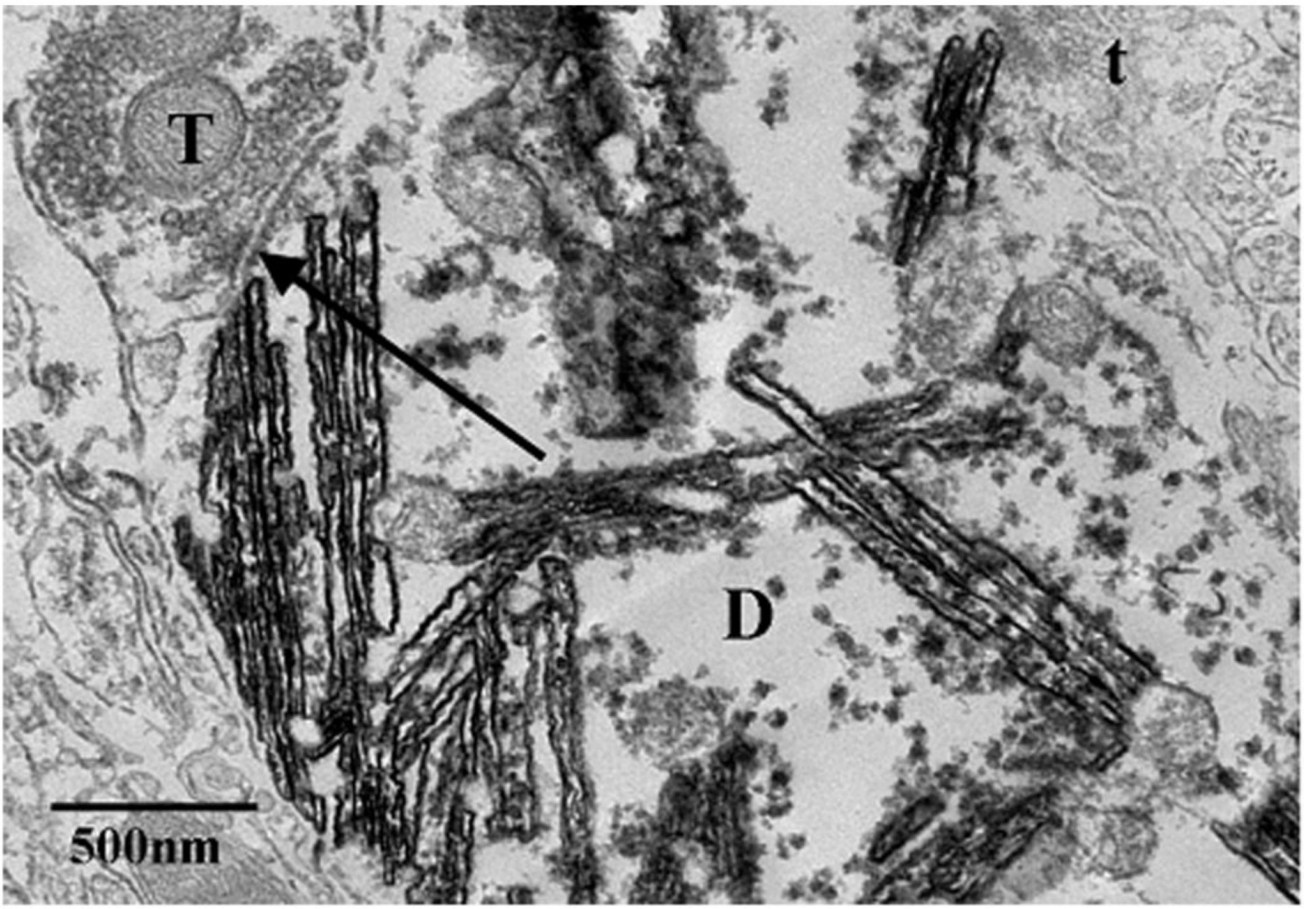

Figure 2.

Axo-dendritic synaptic contacts with dendrites of an antrum projecting neuron in the DMV. An example of a synaptic contact (arrow) between a CTB-HRP-labeled dendrite (D), which was easily identified by dark crystalline TMB-tungstate reaction product, and a GAD67-IR terminal (T) containing the DAB-reaction product. Unlabeled terminals are also identified (t) for comparison. Note that the GAD67-IR terminal (T) contains a population of small, clear, round vesicles.

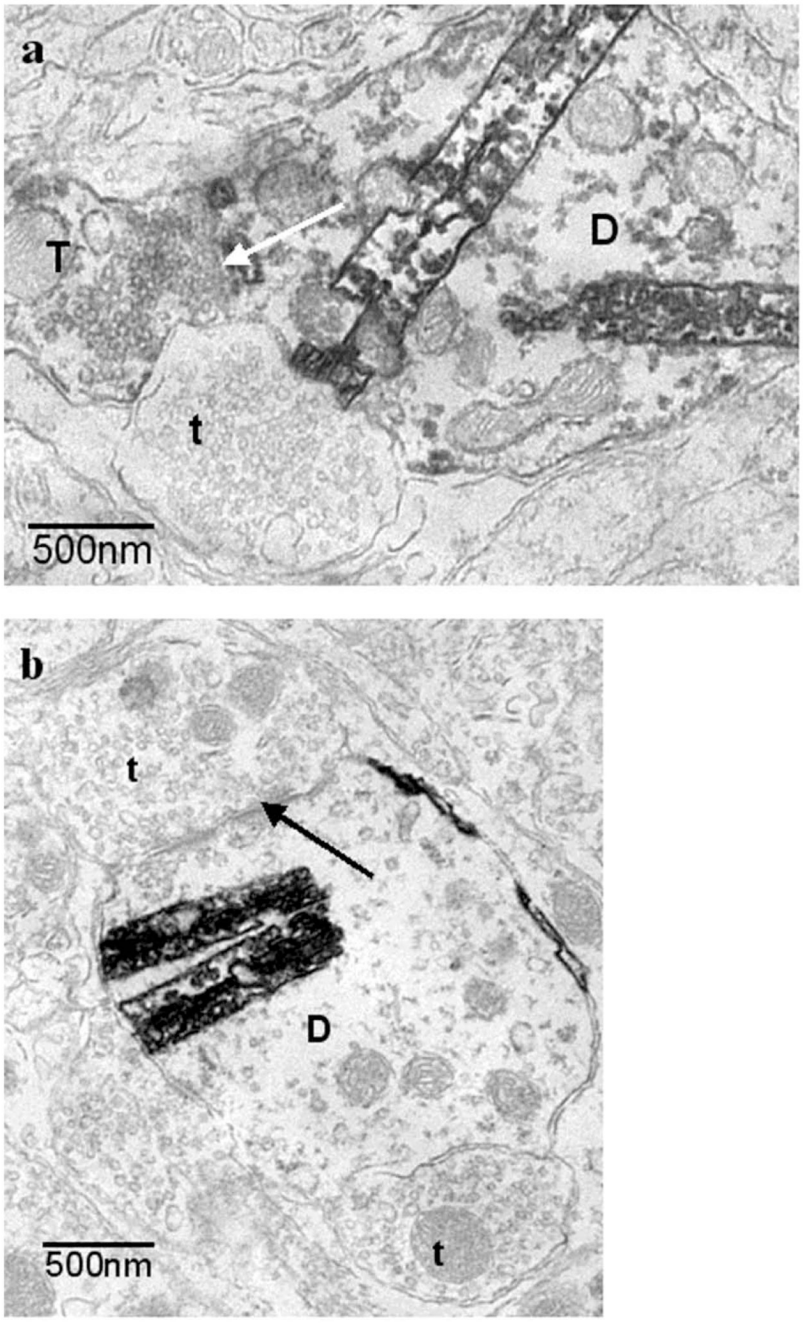

Figure 3.

Axo-dendritic synaptic contacts with dendrites of a fundus projecting neuron in the DMV. 3a) example of synaptic contact (white arrow) between a CTB-HRP-labeled dendrite (D), which was easily identified by dark crystalline TMB-tungstate reaction product, and a GAD67-IR terminal (T) containing the DAB-reaction product. Unlabeled terminals are also identified (t) for comparison. Note that the GAD67-IR terminal (T) contains a population of small, clear, round, vesicles. 3b) Many synaptic contacts also existed between antrum projecting CTB-HRP-labeled dendrites and unlabeled terminal (t).

Table 1

Summary of the Ultrastructural Analysis of GAD_{67}-IR Terminals Forming Synaptic Contacts with DMV Neurons

Area injected with CTβ-HRP	Number of Retrogradely Labeled Profiles Examined	Total Synaptic Contacts with Retrogradely Labeled Profiles	Percent of Synapses Formed with Immunoreactive Terminals	Total Appositions with Retrogradely Labeled Profiles	Percent of Appositions with Immunoreactive Terminals
Antrum	195	214	23.0 +/− 3.6%	78	19.9 +/− 6.3 %
Fundus	203	220	7.9 +/− 3.1%	118	17.4 +/− 3.4 %